Z. Phys. D – Atoms, Molecules and Clusters 18, 17–24 (1991)

Atoms, Molecules and Clusters
Zeitschrift für Physik D

Mechanical Hanle effect

R. Kaiser, N. Vansteenkiste, A. Aspect, E. Arimondo*, and C. Cohen-Tannoudji

Laboratoire de Spectroscopie Hertzienne de l'Ecole Normale Supérieure** and Collège de France, 24 rue Lhomond, F-75231 Paris Cedex 05, France

Received 6 September 1990

Abstract. This paper describes an experiment where the Hanle effect in the ground state of an atomic transition is detected, not by a modification of the light absorbed or reemitted by the atoms, but by a modification of the atomic trajectories. The experimental results are compared with the theoretical predictions of two calculations, the first one considering only the steady-state regime, the second one including the effects of the transient phenomena which take place when the atom enters the laser beam.

PACS: 32.80.B; 32.80.P

1. Introduction

It is a great pleasure for us to dedicate this paper to Professor W. Hanle and to show him a new manifestation of the effect which he discovered more than sixty years ago [1] and which has played such an important role in Atomic Physics.

The Hanle effect can, very generally, be considered as resulting from the competition between two perturbations with different symmetries: a Larmor precession around a static magnetic field B applied along the direction n; an optical excitation produced by a light beam having a polarisation e_L which is not invariant by rotation around n. In zero magnetic field, there is no Larmor precession, and the anisotropy (orientation or alignment) introduced in the atomic state by the light beam can build up. When the magnetic field is applied, the anisotropy introduced by the light beam along a direction transverse to n starts to precess around n with a Larmor frequency $\Omega_B = \gamma B$ proportional to B (γ: gyromagnetic ratio of the atomic state). Such a precession will wash out the anisotropy transverse to n if, during the characteristic damping time τ of the atomic state (radiative lifetime for an atomic excited state, optical pumping time or relaxation time for an atomic ground state), the rotation angle $\Omega_B \tau$ is not small compared to 1. It follows that, when B is scanned around zero, the anisotropy introduced by the light beam in the atomic state undergoes resonant variations which can be detected by changes in the light absorbed or emitted by the atoms. The corresponding resonances, called Hanle resonances (or zero-field level crossing resonances since they are centred on the value zero of the magnetic field for which all Zeeman sublevels cross), have a width ΔB given by

$$\gamma \Delta B = 1/\tau \tag{1}$$

Hanle resonances in atomic ground states were observed for the first time in 1964 [2]. Their interest lies in the fact that the damping time τ for atomic ground states can be much longer than the radiative lifetime of excited states, so that the width ΔB can be extremely small. For example, for ^{87}Rb atoms contained in a paraffin coated cell, τ can be as long as 1 second, which leads (with $\gamma \simeq 1$ MHz/Gauss) to widths ΔB of the order of 1 microgauss. Very sensitive magnetometers, able to detect fields smaller than 10^{-9} Gauss, have been developed in this way [3, 4].

During the last fifteen years, it has been realized that the mechanical effects of light, resulting from resonant exchanges of linear momentum between atoms and photons, can lead to spectacular effects [5]. The purpose of this paper is to show that the Hanle effect in atomic ground states can give rise to a modification of the atomic trajectories when a static magnetic field, perpendicular to the laser polarisation, is scanned around zero.

We first present in Sect. 2 a simple explanation of the physical effect, allowing us to point out differences which exist between the optical and mechanical detections of the Hanle effect. Using a semiclassical approach, we then evaluate in Sect. 3, for the simplest possible atomic transition having a degenerate atomic ground state ($J_g = 1/2 \leftrightarrow J_e = 1/2$), the steady-state atomic density

* Permanent address: Dipartimento di Fisica, Universita di Pisa, I-56100 Pisa, Italy

** Laboratoire associé au Centre National de la Recherche Scientifique et à l'Université Pierre et Marie Curie

matrix, from which it is possible to derive the expression of the mean force deflecting the atomic beam as a function of the magnetic field. Our experimental results, obtained on the transition $2^3S_1 \leftrightarrow 2^3P_1$ of ^{4}He, are presented in Sect. 4 and compared with the theoretical predictions of Sect. 3. Such a comparison shows that one cannot in general neglect the photons absorbed during the transient regime which takes place when the atom enters the laser beam. We thus present in Sect. 5 a more precise description of the phenomena, which takes into account the transient regime and which corresponds to the level scheme studied experimentally (transition $J_g = 1 \leftrightarrow J_e = 1$).

2. Presentation of the effect in a simple case

The principle of the experiment is the following (see Fig. 1a). An atomic beam, propagating along the Ox axis, is irradiated at right angle by a resonant σ^+ polarized laser beam propagating along Oz. In this section, we consider the simple case where the laser excites a $(J_g = 1/2 \leftrightarrow J_e = 1/2)$ transition (see Fig. 1b which gives the Clebsch-Gordan coefficients of the various components of the optical line). A static magnetic field B is applied along Oy and slowly scanned around zero.

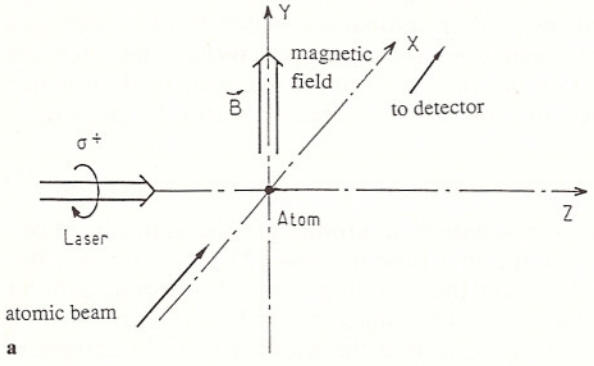

a

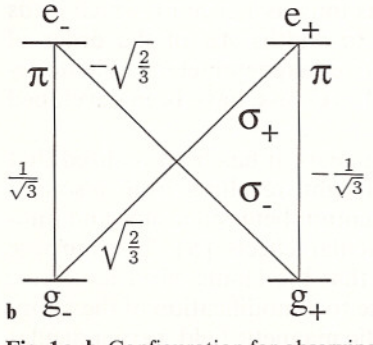

b

Fig. 1a, b. Configuration for observing the mechanical Hanle effect: **a** Experimental configuration: the laser beam is applied transversely to the atomic beam, and can deflect the atoms. This deflection, measured by the detector, exhibits a resonant variation when the transverse magnetic field is scanned. **b** Simplest atomic level scheme for observation of the mechanical Hanle effect with a σ_+ circularly polarized laser. At zero magnetic field, the atoms are optically pumped into g_+ where they no longer interact with the laser, and there is no deflection. We have indicated the Clebsch-Gordan coefficients characterizing the strength of the transitions

Suppose first that one measures the absorption of the light beam by the atoms. Let us take Oz as a quantization axis and let $|g_+\rangle$ and $|g_-\rangle$ be the eigenstates of J_g with eigenvalues $+\hbar/2$ and $-\hbar/2$. Since there is no σ^+ transition starting from $|g_+\rangle$ (see Fig. 1b), the absorption of the σ^+ polarized laser beam is proportional (at low intensity) to the population of $|g_-\rangle$.

As a result of optical pumping by the σ^+ polarized laser beam, each atom crossing the interaction zone is transferred from the sublevel $|g_-\rangle$ to the sublevel $|g_+\rangle$. Just after such an optical pumping cycle, its spin points along the positive direction of the Oz axis. Then it starts to precess around the magnetic field with an angular frequency Ω_B proportional to B. If $B=0$, there is no Larmor precession and the atom remains in the state $|g_+\rangle$, so that the absorption vanishes. When B is non zero, the Larmor precession around Oy induces a Rabi oscillation between $|g_+\rangle$ and $|g_-\rangle$, which repopulates the state $|g_-\rangle$ and therefore gives rise to a non zero absorption. Such an absorption remains small as long as the spin rotates by a small angle before undergoing a new optical pumping cycle which puts it back into the state $|g_+\rangle$, i.e. as long as $\Omega_B \tau_P \ll 1$, where τ_P is the optical pumping time. On the other hand, when B is large enough, so that $\Omega_B \tau_P \gg 1$, the two sublevels $|g_+\rangle$ and $|g_-\rangle$ are completely mixed by the Larmor precession, the population of $|g_-\rangle$ is equal to 1/2 and the absorption takes a large value. One therefore expects the absorption of the light beam, plotted versus B, or Ω_B, to exhibit a narrow dip centred on $\Omega_B = 0$, with a width given by $\Delta\Omega_B \approx 1/\tau_P$. What we have described is just an optical detection of the Hanle effect in an atomic ground state.

Consider now what happens to the atomic trajectory. After each fluorescence cycle, consisting of an absorption of a laser photon followed by a spontaneous emission, the atom gets a momentum kick equal, on the average, to $+\hbar k$ along Oz. This is due to the fact that the momentum of the absorbed photon is always the same ($+\hbar k$ along Oz), whereas the momentum loss due to spontaneous emission is zero on the average since spontaneous emission can occur in a random direction, but with equal probabilities in two opposite directions. When $B=0$, each atom undergoes a very small number of fluorescence cycles before being optically pumped into the sublevel $|g_+\rangle$ where it remains trapped. The momentum transfer along Oz is then limited to a few $\hbar k$ and consequently the deflection of the atomic trajectory remains very small. On the other hand, when B is large, optical pumping cannot empty the sublevel $|g_-\rangle$ since it is refilled at a much faster rate by the Larmor precession around Oy. The absorption of photons by the atom then never stops during its transit time through the laser beam, producing a large momentum transfer along Oz, and consequently a large deflection of the atomic trajectory. The critical value of the field, for which the effects of optical pumping and Larmor precession are on the same order, is still given by (1), so that one expects to get, for the variations of the deflection versus B, the same type of curve as the one obtained for the optical detection of the Hanle effect.

Although they look quite similar, the optical and mechanical detections of the Hanle effect differ in some important respects. First, the atomic trajectory keeps a record of all fluorescence cycles, since each absorbed photon transfers a momentum $+\hbar k$ along Oz, so that the deflection of each atom reflects the integral of the force experienced by such an atom during the whole interaction time, including the transient regime. By contrast, the optical detection signal can give local informations on the state of the atom at the point of observation. Second, the mechanical detection does not introduce any extra fluctuation. The random nature of the deflection is only related to the fundamental fluctuations of the number of fluorescence cycles occurring during a given time interval and to the random direction of the spontaneously emitted photons. By contrast, an additional statistical element has to be considered for optical signals, namely the fact that each photon is usually not detected with a 100% efficiency [6]. Third, the atomic detectors may be much more efficient that photodetectors. For instance, the lower state of the atomic transition of Helium which we have studied is a metastable state, carrying a lot of internal energy, so that it is very easy to detect the deflected atoms with an electron multiplier. By contrast, the fluorescence photons have a wavelength equal to 1.08 μm not convenient to detect with current photomultipliers. Finally, if one wants to make quantitative comparisons between experimental data and theoretical predictions, the mechanical detection signals do not require absolute calibrations of quantities such as mean number of photons, detector efficiency, probe intensity .... An example of such advantages will clearly appear in Sect. 4.

3. Calculation of the steady-state force

3.1. Principle of the calculation

In this section, we compute the mean force experienced by the atom in the steady-state regime. We use the so-called semiclassical approximation which is valid when the spatial extension of the atomic wave packet is small compared to the laser wavelength [7, 8]. The mean radiative force can then be written

$$f(r) = -\langle \nabla V_{AL}(r) \rangle \tag{3.1}$$

where

$$V_{AL}(r) = -d \cdot E_L(r) \tag{3.2}$$

is the electric dipole interaction hamiltonian describing the coupling between the atomic dipole moment d and the laser electric field $E_L(r)$, treated as a c-number external field and evaluated at the center of the atomic wave packet. The quantum average value appearing in (3.1) involves only the internal degrees of freedom, so that f can be expressed in terms of the atomic density matrix σ describing the internal atomic state. To calculate σ, we use the so-called optical Bloch equations which describe the evolution of σ, including the hamiltonian evolution in the external laser and magnetic fields as well as the damping due to spontaneous emission.

We consider here a $J_g = 1/2 \leftrightarrow J_e = 1/2$ transition (see Fig. 1 b). Since we are only interested in the Hanle resonance of the ground state, which is much narrower than the Hanle resonance of the excited state, we consider a simplified model where the gyromagnetic ratio γ_e of the excited state is zero. This simplification does not affect the shape of the narrow structure appearing in the detection signal (Hanle effect in the ground state), but this model cannot of course give a precise account of the broader structures. Since the laser light excites only the $|e_+\rangle$ Zeeman sublevel, which cannot be coupled to $|e_-\rangle$ because of the previous assumption ($\gamma_e = 0$), we can ignore $|e_-\rangle$. The total hamiltonian H describing the atom in the external laser and magnetic fields is thus

$$H = \hbar\omega_0 |e_+\rangle\langle e_+| + V_{AL} + V_B \tag{3.3}$$

In (3.3), $\hbar\omega_0$ is the energy interval between e and g, V_{AL} is given in (3.2) and

$$V_B = -i\hbar \frac{\Omega_B}{2} |g_-\rangle\langle g_+| + h.c. \tag{3.4}$$

describes the Zeeman coupling of the atomic ground state with a magnetic field B applied along Oy (Larmor frequency $\Omega_B = -\gamma_g B$).

For a σ^+ polarized laser wave propagating along Oz, the laser electric field is

$$E_L(z,t) = E_0 \, \varepsilon_+ \exp i(k_L z - \omega_L t) + c.c. \tag{3.5}$$

where $\varepsilon_+ = -(\varepsilon_x + i\varepsilon_y)/\sqrt{2}$. In the so-called rotating wave approximation, V_{AL} can be written

$$V_{AL} = \frac{\hbar\Omega_L}{2} |e_+\rangle\langle g_-| \exp i(k_L z - \omega_L t) + h.c. \tag{3.6}$$

where

$$\Omega_L = -\langle e_+ | \mathbf{d} \cdot \boldsymbol{\varepsilon}_+ | g_- \rangle E_0/\hbar \tag{3.7}$$

is the Rabi frequency characterizing the atom-laser coupling. We suppose that the atom, moving along Ox, crosses the laser beam at $z = 0$, which leads for the mean force f to the following expression

$$f = -\langle \nabla V_{AL}(z=0) \rangle = i\hbar k_L e_g \frac{\Omega_L}{2} \sigma_{e_+ g_-} \exp i\omega_L t + c.c. \tag{3.8}$$

The value of the density matrix elements $\sigma_{e_+ g_-}$ is determined from the optical Bloch equations

$$\frac{d\sigma}{dt} = \frac{1}{i\hbar}[H, \sigma] + \left(\frac{d\sigma}{dt}\right)_{sp} \tag{3.9}$$

where H is given in (3.3), and where the damping terms due to spontaneous emission have the following expression

$$(d\sigma_{e_+ e_+}/dt)_{sp} = -\Gamma \sigma_{e_+ e_+}$$

$$(d\sigma_{e_+ g_i}/dt)_{sp} = -\frac{\Gamma}{2}\sigma_{e_+ g_i}$$

$$(d\sigma_{g_+ g_+}/dt)_{sp} = +\frac{\Gamma}{3}\sigma_{e_+ e_+}$$

$$(d\sigma_{g_- g_-}/dt)_{sp} = +\frac{2\Gamma}{3}\sigma_{e_+ e_+}$$

$$(d\sigma_{g_+ g_-}/dt)_{sp} = 0 \tag{3.10}$$

where $i = -, +$ and where Γ^{-1} is the radiative lifetime of e. If we put

$$\tilde{\sigma}_{e_+ g_i} = \exp i\omega_L t \sigma_{e_+ g_i} \tag{3.11}$$

the optical Bloch equations take the form of a set of coupled linear differential equations with time independent coefficients. For example, the equation of evolution of $\tilde{\sigma}_{e_+ g_-}$ is

$$\dot{\tilde{\sigma}}_{e_+ g_-} = i\left(\delta + i\frac{\Gamma}{2}\right)\tilde{\sigma}_{e_+ g_-} + \frac{i\Omega_L}{2}(\sigma_{e_+ e_+} - \sigma_{g_- g_-}) - \frac{\Omega_B}{2}\tilde{\sigma}_{e_+ g_+} \tag{3.12}$$

where

$$\delta = \omega_L - \omega_0 \tag{3.13}$$

is the detuning between the laser frequency and the atomic frequency.

3.2. *Steady-state solution*

The laser-atom interaction time is the time $T = l/v$ it takes for the atom with velocity v to cross the laser beam diameter l. We will suppose that T is long enough for allowing the atom to reach a steady-state. On the other hand, T is supposed to be not too long, so that one can neglect the Doppler effect associated with the mean velocity Δv_g communicated by the laser to the atom during the interaction time

$$k_L \Delta v_z \ll \Gamma \tag{3.14}$$

One can thus consider that the detuning (3.13) between the laser frequency and the atom frequency remains constant during T. The steady-state solution of optical Bloch equations can then be calculated analytically. Inserting the corresponding value of $\sigma_{e_+ g_-}$ into (3.8), one gets the following expression for the steady-state force

$$f_{st} = \hbar k_L \frac{\Gamma}{2} \frac{\frac{\Omega_L^2}{4}}{\delta^2 + \frac{\Gamma^2}{4} + \frac{\Omega_L^2}{6} + \frac{\Omega_B^2}{4}\left(1 + \frac{\Omega_L^4}{6\Omega_B^4}\right)} \tag{3.15}$$

In Fig. 2, we have plotted this force versus Ω_B, for $\Omega_L = 0.2\Gamma$ and for a zero detuning. The dip which appears around $\Omega_B = 0$ is a signature of the Hanle effect in the ground state. The decrease of f_{st} for larger values of Ω_B is due, in the simplified model use here ($\gamma_e = 0$), to the fact that the laser excitation gets out of resonance when the Zeeman shift of the ground state sublevels becomes of the order of Γ. In a more precise treatment ($\gamma_e \neq 0$), such a decrease would also be partly associated with the Hanle effect in the excited state.

Here we are only interested in the central dip of Fig. 2 and in the low intensity limit ($\Omega_L \ll \Gamma$) where this dip is very narrow, with a width $\Delta\Omega_B \ll \Gamma$. Putting $\delta = 0$ in the denominator of (3.15) and neglecting $\Omega_L^2/6$ and $\Omega_B^2/4$ in comparison with $\Gamma^2/4$, one easily transforms (3.15) into

$$f_{st} = \hbar k_L \frac{\Gamma}{2}\frac{\Omega_L^2}{\Gamma^2}\left[1 - \frac{\Gamma'^2}{\Omega_B^2 + \Gamma'^2}\right] \tag{3.16}$$

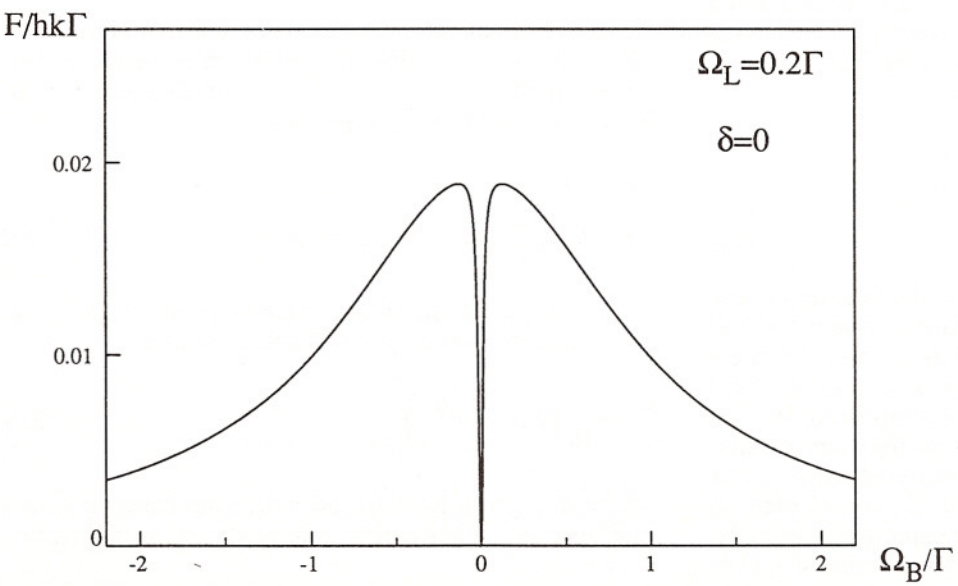

Fig. 2. Mechanical Hanle effect: This curve presents the result of the calculation of Sect. 3, and shows the value of the steady state force as a function of the Larmor angular frequency of precession in the ground state. The narrow resonance around 0 is the manifestation of the Mechanical Hanle effect

where

$$\Gamma' = \frac{\Omega_L^2}{\Gamma\sqrt{6}} \tag{3.17}$$

It is clear on (3.16) that the narrow dip goes to zero for $\Omega_B = 0$ and has a Lorentzian shape with a width $2\Gamma'$. Moreover, one recognizes in Γ' the absorption rate of laser photons from the ground state (at resonance and at low intensity), or equivalently the inverse of the optical pumping time. The calculations of this section thus confirm the qualitative predictions of Sect. 2 according to which the width of the Hanle resonance of the ground state must be equal to the inverse of the optical pumping time.

4. Experimental results

4.1. Apparatus

The experimental setup (Fig. 3a) is the same as the one used for other experiments [9–11]. The atomic source is a supersonic beam of Helium cooled by liquid nitrogen, and excited by colinear electron bombardment. After elimination of undesirable atomic species, we have a beam of triplet metastable 2^3S_1 propagating along Ox. The velocity distribution is peaked at 1300 ms^{-1}, and has a width ΔV of 150 ms^{-1} (HWHM).

The atoms interact with a circularly polarized transverse laser beam, propagating along Oz, tuned on the $2^3S_1 - 2^3P_1$ transition ($\lambda = 1.083$ μm; natural linewidth $\Gamma/2\pi = 1.6$ MHz) (Fig. 3b). The home built LNA laser [11] is frequency stabilized to 0.1 MHz. The beam is enlarged (beam waist radius 50 mm) in order to have an almost uniform intensity on the interaction region 40 mm long, determined by a diaphragm. The intensity (0.6 $mWcm^{-2}$) corresponds to a Rabi angular frequency $\Omega_L = \Gamma$ for any σ_+ component of the considered transition (Fig. 3b). The magnetic field in the interaction region is controlled by three pairs of coils, approximately in the Helmholtz position, allowing us to achieve an inhomogeneity less than 10^{-3} on the interaction volume.

In order to measure the transverse velocity distribution, we limit the atomic beam by a slit S_1, 0.2 mm wide along Oz, placed just before the interaction region. The transverse atomic beam profile is scanned along Oz by an electron multiplier with a similar input slit, placed 1.3 m after the interaction region. This detector is sensitive only to the metastable atoms. Because of the narrow longitudinal velocity distribution, we obtain directly the transverse velocity distribution, with a resolution of 0.1 ms^{-1} (HWHM) in the range ± 10 ms^{-1}. Comparing these profiles with and without the laser allows us to observe the deflection of the atoms.

4.2. Direct observation of the mechanical Hanle effect

If we place the detector in the far wing of the transverse beam profile, the signal increases with the deflection, and thus with the force experienced by the atoms (Fig. 4). When we scan the transverse magnetic field B_y around 0, we observe the signal of Fig. 5, which clearly shows the dip corresponding to the decrease of the force at $B_y = 0$, as predicted by the analysis above.

This method has allowed us to achieve a compensation of the earth magnetic field in the interaction region exactly along the atomic trajectory. An extension of the calculation of Sect. 3 predicts that the dip is narrower when the components of the magnetic field orthogonal to the one which is scanned are smaller. With an iterative procedure, it is then possible to cancel the three components of the earth magnetic field [12]. When this is done, the width of the dip (10^{-1} Gauss, HWHM) is only due to the absorption rate Γ' (3.17). It is possible to adjust the current in the compensating coils with an accuracy of one tenth of this width, so that we estimate that the earth magnatic field is cancelled to less than 10 mG.

The method above of direct observation of the mechanical Hanle effect does not allow one an accurate comparison between the experiment and the theoretical analysis of Sect. 3. As a matter of fact, the signal is sensitive not only to the average force experienced by the atoms, but also to the spread of the atomic velocity distribution due to the fluctuations of the force: the signal

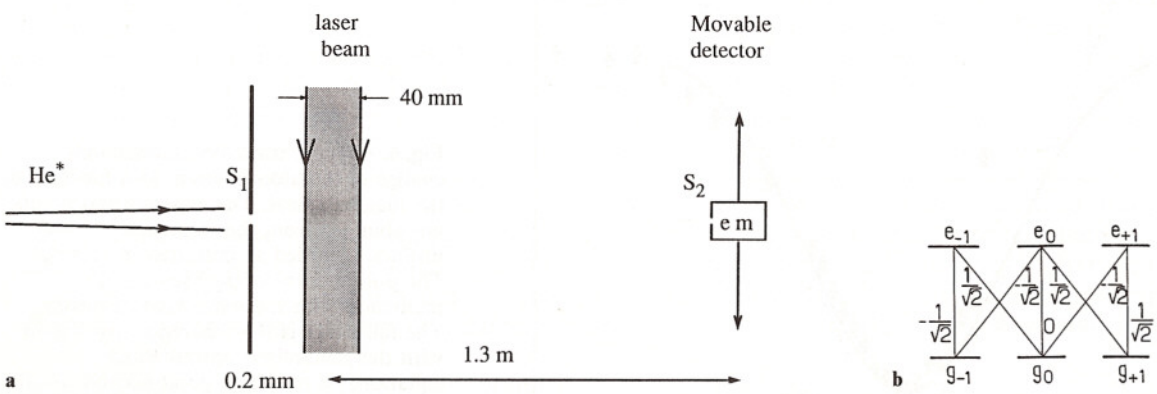

Fig. 3a, b. Experiment: **a** Experimental setup. The metastable beam of helium, transversely limited by the slit S_1 (0.2 mm wide), is analysed by an electron multiplier with a similar slit S_2 yielding the transverse velocity profile. When the laser beam is applied, the atomic beam is deflected, and the transverse velocity profile is modified. **b** Transition of the metastable Helium used for the experiment, with the corresponding Clebsch-Gordan coefficients. Note that the $g_0 \to e_0$ transition is forbidden

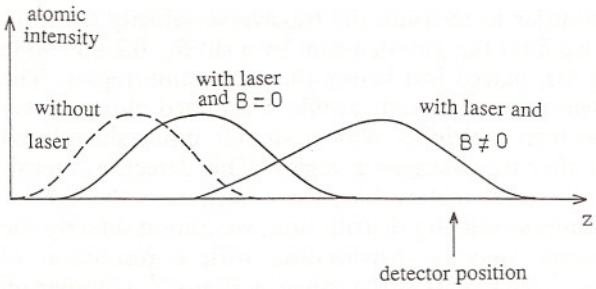

Fig. 4. Direct detection of the Mechanical Hanle Effect: The detector is placed in the far wing of the atomic beam profile, so that the signal increases when the deflection increases

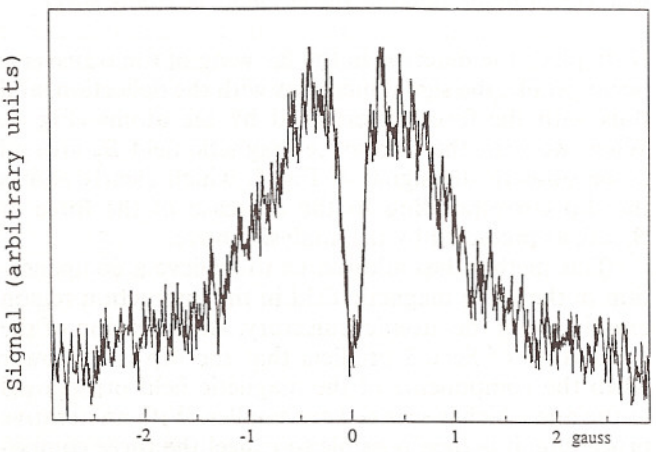

Fig. 5. Direct detection of the Mechanical Hanle Effect: signal obtained with the detector located as indicated in Fig. 4

in the wing of the profile can then increase even if the average force is null. In order to make a quantitative comparison with the theory, we have used another observation method that we describe now.

4.3. Study of the velocity distribution

The method consists of measuring the final velocity distribution for a series of different values of the magnetic field. For each profile, it is then easy to calculate the average velocity. On Fig. 6, we have plotted this average velocity as a function of the magnetic field. We clearly see the dip around zero, characteristic of the magnetic Hanle effect in the ground state.

The dotted line represents the expected average velocity change, calculated by assuming that the steady state force is applied during the whole interaction time of $310\Gamma^{-1}$. The calculation is analogous to the one of Sect. 3, extended to the $J_g=1 \rightarrow J_e=1$ transition of the experiment (Fig. 3b). Although there is a qualitative agreement, we clearly see two quantitative differences. First, the measured velocity change does not go to zero. Second, for a magnetic field B larger than 50 mG, the measured velocity change is smaller than the calculated value.

The difference at large magnetic field is not surprising. The deviation between the calculation and the experiment happens for magnetic fields such that the velocity change is larger than $15\hbar k/M$. The corresponding Doppler effect is then of the order of Γ, and the velocity change is large enough so that the atoms get out of resonance (the condition 3.14 is no longer fulfilled). Note also that our model ignores the Hanle effect in the excited state, but this effect plays little role at these values of the magnetic field (the width of the Hanle effect in the excited state would be of the order of 1 Gauss).

We attribute the difference around zero to the transient regime, which has been ignored in the calculation. The effect of this transient regime can be easily understood at zero magnetic field, where the average steady state force is zero. In fact, if we start with a statistical mixture of atoms equally distributed in the three sublevels of the ground state, it requires several fluorescence

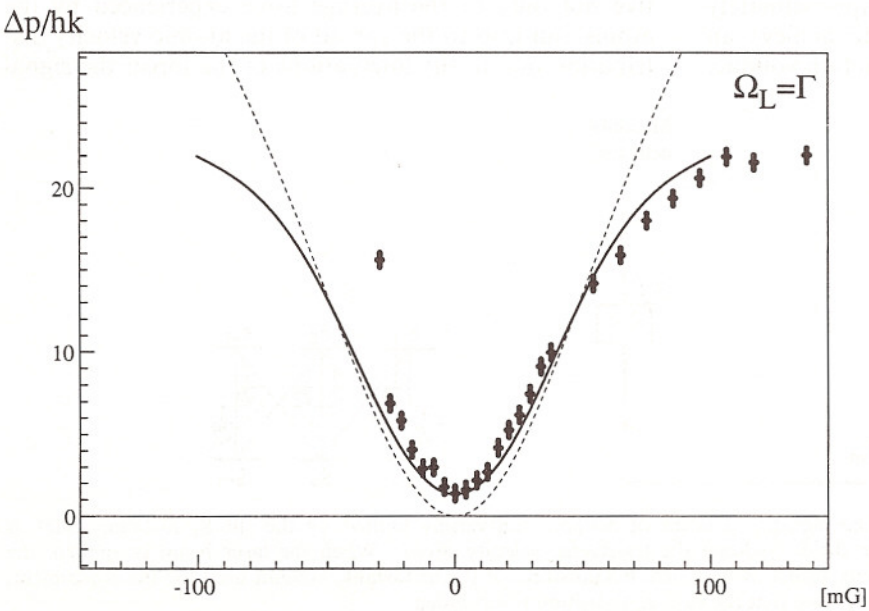

Fig. 6. Average transverse momentum change of the atomic beam, as a function of the magnetic field. The experimental points are obtained from the transverse velocity profiles, recorded as indicated in Sect. 4.2. The dotted curve is the theoretical prediction with the semi-classical theory. The full curve is the theoretical prediction with the generalized optical Bloch equations: it renders a good account of the transient regime (change of $4/3\hbar k$ at zero magnetic field) and of the shape of the wings at larger magnetic field

cycles until all atoms are pumped into the trapping $m_z = 1$ sublevel. A straightforward calculation shows that the average number of fluorescence cycles per atom is

$$\bar{n} = \frac{4}{3} \tag{4.1}$$

This corresponds precisely to the experimentally observed velocity change at zero magnetic field (Fig. 6)

$$\Delta v_0 = 1.3 \hbar k / M \tag{4.2}$$

The theoretical analysis of Sect. 3 is thus unable to give a full quantitative account of the effect: it neglects the variation of the Doppler effect during the deflection, and it does not take into account the transient regime. The transient regime only involves a small number of photons (see above), but the sensitivity of the method is large enough to measure such small velocity changes (Fig. 6).

We will present now a completely different theoretical analysis to take into account these effects.

5. Full quantum treatment

In order to render a better account of the experimental results, one possibility would be to try to improve the semiclassical calculation of Sect. 3 by including the transient regime and the velocity change during the interaction time. We have found more fruitful to use another approach, starting directly from the full quantum equations where both the internal and external degrees of freedom of the atom are quantized [14]. The numerical intergration of these equations gives us directly the time dependent atomic density matrix from which we compute the velocity distribution by tracing over the internal variables. Also, it turns out that this fully quantum approach is more correct when the atomic velocity (along Oz) is so small that the corresponding de Broglie wavelength is no longer negligeable compared to the laser wavelength.

This theoretical treatment is very close to the one used to describe laser cooling below the one-photon recoil energy by velocity selective coherent population trapping [9, 13]. Let us introduce the state $|g_-, p_z\rangle$, which represents the atom in the ground state g_- with a linear momentum p_z along Oz. Because of the selection rule for the angular momentum, the σ^+ polarized wave can couple together only g_- and e_+. On the other hand, because of the selection rule for the linear momentum, such an interaction with a wave propagating towards $+Oz$ can couple only $|g_-, p_z\rangle$ and $|e_+, p_z + \hbar k\rangle$. The magnetic field along Oy couples the different Zeeman levels in the ground state $|g_-, p_z\rangle$ and $|g_+, p_z\rangle$ without modifying their linear momentum. Assuming a zero gyromagnetic factor in the excited state $\gamma_e = 0$, we are thus led to introduce a family of three states coupled by absorption or stimulated emission and by the static magnetic field:

$$F(p_z) = \{|g_-, p_z\rangle, |g_+, p_z\rangle, |e_+, p_z + \hbar k\rangle\} \tag{5.1}$$

As long as spontaneous emission is not taken into account, this is a closed family of coupled states. Taking into account the spontaneous emission of photons gives rise to a redistribution between different families: an atom in the state $|e_+, p_z + \hbar k\rangle$ from the family $F(p_z)$ can emit a photon with a linear momentum u along $Oz (|u| \leqq \hbar k)$ and arrive into $|g_-, p_z + \hbar k - u\rangle$ which belongs to $F(p_z + \hbar k - u)$.

Considering such families of states introduces significant simplifications in the equations of evolution of the atomic density matrix (generalized optical Bloch equations, including the external quantum number p_z, see [13]). We have numerically solved these equations, using a truncation and a discretisation of p_z similar to the one described in [13]. From the result of this numerical integration we get the value of the density matrix as a function of time. We then deduce the final atomic linear momentum distribution $N(p_z)$ along Oz, which can be written:

$$N(p_z) = \langle g_-, p_z | \sigma | g_-, p_z \rangle + \langle g_+, p_z | \sigma | g_+, p_z \rangle + \langle e_+, p_z | \sigma | e_+, p_z \rangle \tag{5.2}$$

The curve in full line of Fig. 6 represents the results of the computation done for the $J_g = 1 \to J_e = 1$ transition of Helium excited by a σ_+ transition, corresponding to our experimental parameters ($\delta = 0$, $\Omega_L = \Gamma$, $T = 310 \Gamma^{-1}$). Such a curve obtained without any adjustable parameter is in a very good quantitative agreement with the experimental results. Note in particular the change of $\Delta p = \frac{4}{3} \hbar k$ in linear momentum for $B = 0$, and the reduced slope of the curve for large values of B. We thus see that the calculation sketched in this section, which relies on a completely rigourous approach of the problem, gives results in excellent agreement with the experimental data. It contains other informations, for instance about the spread of the velocity distribution, that could also be compared to the measurements. It is clearly a very powerful theoretical method.

6. Conclusion

We have presented in this paper a new manifestation of the Hanle effect in an atomic ground state. The effect appears as a resonant modification of the atomic trajectories in an atomic beam irradiated transversely by a laser, when the magnetic field is scanned around 0. The sensitivity of the method has allowed us to detect effects corresponding to a single fluorescence cycle. At this level of precision, semi-classical models are no-longer adequate. We have thus presented a fully quantum analysis, where internal and external degrees of freedom of the atom are quantized. This analysis provides an accurate quantitative interpretation of the experimental results without any adjustable parameter.

References

1. Hanle, W.: Z. Phys. **30**, 93 (1924); Z. Phys. **35**, 346 (1926)
2. Lehmann, J.-C., Cohen-Tannoudji, C.: C. R. Acad. Sci. **258**, 4463 (1964)

3. Dupont-Roc, J., Haroche, S., Cohen-Tannoudji, C.: Phys. Letters **28**A, 638 (1969)
4. Cohen-Tannoudji, C., Dupont-Roc, J., Haroche, S., Laloë, F.: Phys. Rev. Letters **22**, 758 (1969)
5. See for example the papers published in the special issue on "Laser cooling and trapping of atoms". Chu, S., Wieman, C. (eds.) J. Opt. Soc. Am. B**6** (1989)
6. Cook R.J. has suggested to use the deflection of an atomic beam for studying the statistics of fluorescence photons without being limited by the efficiency of photodetectors: Cook, R.J.: Opt. Commun. **35**, 347 (1980); see also the experiments described in Wang, Y.Z., Huang, W.G., Cheng, Y.D., Liu, L.: In laser spectroscopy VII. Hansch, T.W., Shen, Y.R. (eds.) p. 238. Berlin, Heidelberg, New York: Springer 1985
7. Cook, R.J.: Phys. Rev. A **20**, 224 (1979)
8. Gordon, J.P., Ashkin, A.: Phys. Rev. A **21**, 1606 (1980)
9. Aspect, A., Arimondo, E., Kaiser, R., Vansteenkiste, N. Cohen-Tannoudji, C.: Phys. Rev. Lett. **61**, 826 (1988)
10. Aspect, A., Vansteenkiste, N., Kaiser, R., Haberland, H., Karrais, M.: Chem. Phys. **145**, 307 (1990)
11. Vansteenkiste, N., Gerz, C., Kaiser, R., Holberg, L., Salomon, C., Aspect, A.: J. Phys. (Paris) (submitted)
12. It is also possible to use a linearly polarized laser beam. One can then show that there is a similar Hanle resonance when the component B_Z of the magnetic field is scanned around 0. See Kaiser, R., thèse de doctorat de l'Université Pierre et Marie Curie (Paris VI), Paris 1990
13. Aspect, A., Arimondo, E., Kaiser, R., Vansteenkiste, N., Cohen-Tannoudji, C.: J. Opt. Soc. Am. B**6**, 2112 (1989)
14. Cook, R.J.: Phys. Rev. A **22**, 1078 (1980)